Theo. Exp. NANOTECHOLOGY 4 (2020) 65-72

Experimental and Theoretical NANOTECHNOLOGY
http://etn.siats.co.uk/

Analysis and characterisation of polycrystalline ZnS nanostructure

*M. C. Benesten, C. J. Thordor, C. Anderson**

Technical University of Denmark, Department of Materials Engineering, Roskilde, Denmark
*Email: cason@dtu.dk

Received: 27/12/2019 / *Accepted:* 25/5/2020 / *Published:* 1/9/2020

Zinc Sulfide (ZnS) thin films were deposited on glass substrates at the pressure of 10-6 mbar by thermal resistor evaporation technique. The effects of annealing on the structural and optical properties of ZnS films were studied. Polycrystalline ZnS films have been analyzed by X-ray diffraction. Only hexagonal phase with the preferred (111) plane was found in ZnS films. Optical characteristics were studied as a function of annealing temperature and film thickness in air. The results show that the energy band gap was found to be about 3.5 eV. It was observed that the energy gap decreases with the increase in the film thickness and increases with the increase in the annealing temperature.

Keyword: ZnS; Optical; Vacuum; Annealing.

1. INTRODUCTION

Zinc sulfide (ZnS) is a wide gap and direct transition semiconductor [1] and belonging to the II-VI group is one of the promising materials for electronic devices. Consequently, it is a potentially important material to be used as an antireflection coating for hetero-junction solar cells [2]. It is an important device material for the detection, emission and modulation of visible and near ultra violet light [3, 4]. In particular, ZnS is believed to be one of the most promising materials for blue light emitting laser diodes [5] and thin film electroluminescent displays [6]. The deposition of ZnS films has become increasingly important due to the widened industrial applications. ZnS has been the subject of intensive research because of its intermediate band gap (3.5 eV) making the material suitable as window material for a hetero-junction solar cell, high absorption coefficient, reasonable conversion efficiency, stability and low cost. Knowledge of the optical properties of ZnS films is very important in the field of optoelectronic devices like photo-detectors.
There are several preparation methods for ZnS films such as vacuum evaporation, sputtering, spray and Pulsed laser deposition. In our work, ZnS films were deposited with vacuum evaporation technique at room temperature. These ZnS films were then submitted to thermal annealing at different temperatures in order to improve their properties. In this paper we report the optical properties of vacuum evaporation prepared ZnS films and their microstructure.

2. EXPERIMENTAL DETAILS

VAS BUC (78535-France) evaporation system was used to prepare ZnS thin films. A tungsten boat was used as a support to evaporate ZnS granule with 99.99% purity. A quartz crystal monitor mounted near the substrate was used for in-*situ* measurement of the thickness of the thin films as well as the evaporation rate, which was kept around 0.3 nm/s at the pressure of about 1.5×10^{-5} mbar. ZnS thin films with a thickness of 200 nm were obtained on cleaned glass substrates with dimensions of 76*mm* × 25*mm*. Samples were annealed in air for an hour at temperatures 100, 200, 300 and 400 °C. XRD measurements were carried out using D8 ADVANCE system from Bruker company, (Anode material: Cu-Cu $k\alpha_1$ line with λ= 1.542Å) of Karaj MERK Institute of Materials and Energy.

3. RESULTS AND DISCUSSION

3.1 XRD measurements

Fig 1. shows the X-ray diffraction patterns of ZnS films without heat treatment and annealed in air at 100, 200, 300 and 400 °C. Diffraction angles and Miller indices of the peaks are shown in figure.

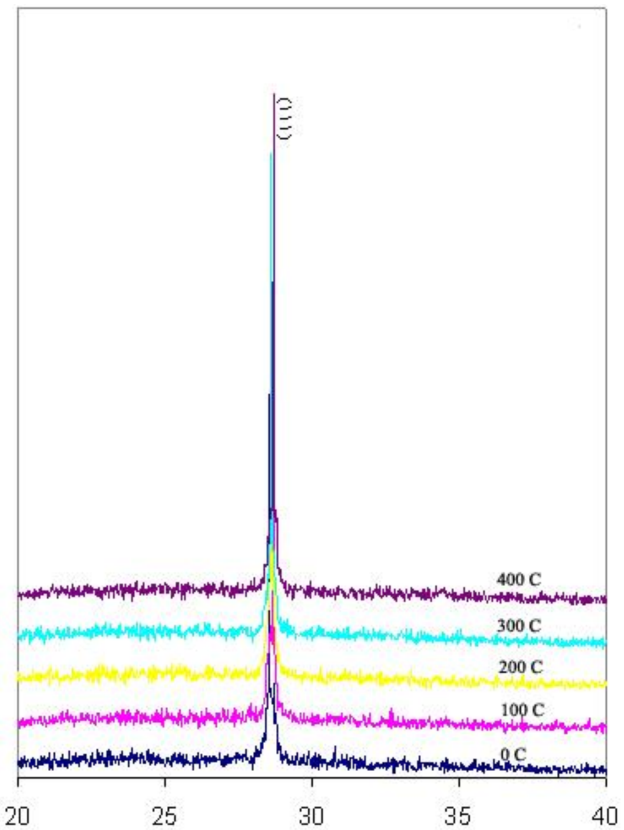

Figure 1 X–ray diffraction patterns of the (111) peaks of the ZnS films as-deposited and annealed at different temperatures

The strong XRD peaks at $2\theta \approx 28.6$ °C correspond to both diffraction angles of the (111) plane of cubic ZnS. Therefore, the ZnS films deposited on a glass substrate by vacuum deposition were of cubic structure and the c-axis of crystallites was mostly oriented perpendicular to the substrate. The grain size of the crystallite (diameter D_{hkl}) was determined from the full width at half maximum ($\Delta\ \omega_{2\Theta}$) of the (111) and peaks by using the Scherer formula [7].

$$D_{hkl}=K\lambda/\beta cos\theta \quad (1)$$

where K is a constant, β the full width at half maximum in radians, λ is the X-ray wavelength and θ is the Bragg's angle. Here K=0.89 for spherical shape (evidence from TEM) [8]. Annealing caused by the rearrangement of ions Zn and S inside the ZnS lattice and to the diffusion of atoms or ions into its volume.

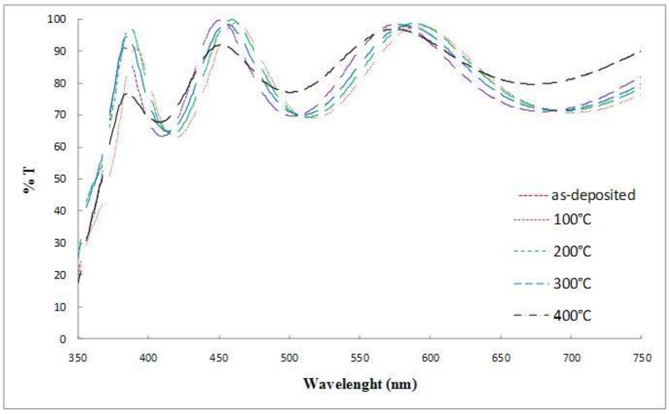

Figure 2 Transmittance versus wavelength of incident radiation for the ZnS thin films as-deposited and annealed at different temperatures.

The values of D_{hkl} were determined according to Fig 2. introduced with presented in Table 1. for ZnS thin films without heat treatment and for annealed samples at 100, 200, 300 and 400 ˚C in air. The largest value of the full width at half maximum at 100 ˚C showed that the size of the crystallites and unit cell volume were minimum at this temperature.

Table 1 Structural properties of ZnS thin films with deposited in 50 °C and grain sizes obtained at different annealing temperatures.

°C	2θ	β	d(A)	a(A)	D(nm)
Nun	28.5968	0.288	7.11482	12.32287	0.497279
100	28.6357	0.336	3.11482	5.394868	0.426276
200	28.6228	0.24	4.11482	7.126868	0.59677
300	28.6273	0.288	5.11482	8.858868	0.497313
400	28.6907	0.24	6.11482	10.59087	0.59686

3.2 Optical measurements

The optical properties of ZnS thin films are determined from transmission and absorbance measurements using double beam automated spectrophotometers (Cintera 101) in the range of wavelength 350–750 nm. Fig. 2. shows the transmission spectra of ZnS thin films deposited at 50 ˚C and annealed in air in varying temperature from 100 to 400 ˚C. The ZnS films showed optical transmission 60- 95 % in the visible range. The absorption coefficient (α) was analyzed using the following expression for near edge optical absorption of semiconductors:

$$\alpha h\upsilon=k(h\upsilon-E_g)^{m/2} \quad (2)$$

where k is constant, E_g is the separation between the valance and conduction bands and m is a constant that is equal to 1 for direct band gap semiconductors. Using the fundamental relations of photon transmission and absorbance,

$$I = I_0 \exp(\alpha t) \quad (3)$$

where t is thickness and

$$A = \log I_0/I \quad (4)$$

we have $\alpha = 2.303A/t$.

The band gap values were determined from the intercept of the straight line portion of the $(\alpha h\upsilon)^2$ against the hυ graph on the hυ-axis using computer fitting program. The linear part shows that the mode of transition in these films is of direct nature. For ZnS films $(\alpha h\upsilon)^2$ versus photon energy, hυ are plotted in Fig. 3. and Fig. 4. The band-gap value was calculated in the range of 2.25–3.35 eV. The band-gap values are lower than bulk value of hexagonal ZnS because of quantum confinement of ZnS nanocrystals which is consistent with the literature [9].

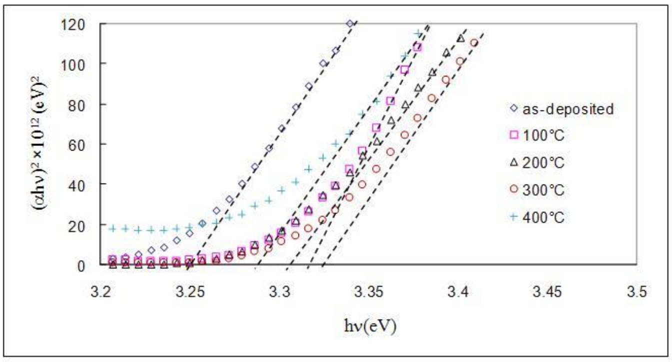

Figure 3 Plot of $(\alpha h\upsilon)^2$ versus photon energy hυ for the ZnS thin films as-deposited and annealed at different temperatures.

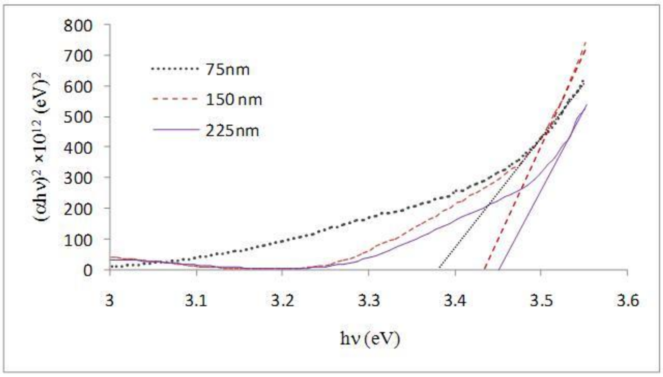

Figure 4 Plot of $(\alpha h\upsilon)^2$ versus photon energy hυ for the ZnS thin films at different thicknesses.

Transmission spectra of the annealed films exhibit a decrease in the optical transmittance with its absorption edge shifted towards the lower wavelength. It is inferred from this that the optical band gap increases on annealing the films.

Fig 5. shows the transmission spectra of hexagonal ZnS thin films in varying thickness from 75 to 225 nm grown on a glass substrate at 50 °C. This figure shows that the films are highly transparent in the visible region. The transmission for the films deposited was 85% between

380 and 800 nm wavelengths, with a minimum of 65% at approximately 550 nm. The sharp absorption edge and high transmission values of the ZnS films at wavelengths >400 nm demonstrates a narrow grain size distribution as well as a low concentration of defects, such as pits and voids in the films [10].

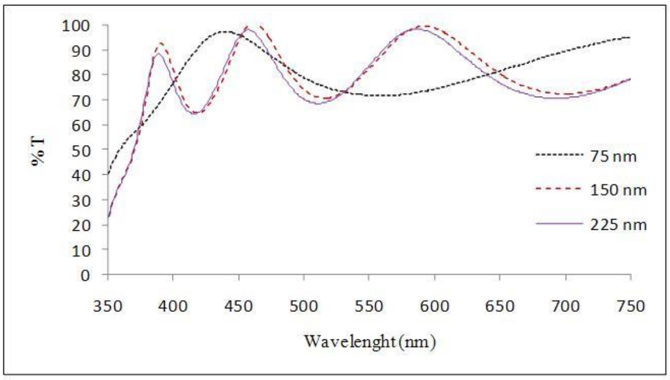

Figure 5 Transmittance versus wavelength of incident radiation for the ZnS thin films at different thicknesses.

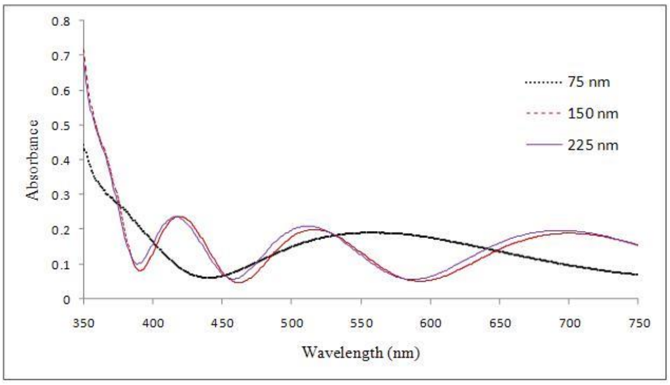

Figure 6 Absorbance versus wavelength of incident radiation for the ZnS thin films at different thicknesses.

The absorbance spectra of the thin films, having different thickness, are shown in Fig 6. These spectra reveal that films, grown under the same parametric conditions have low absorbance in the visible and near infrared regions. However, absorbance in the ultraviolet region is high. The enhanced absorption is observed in the neighborhood of λ = 360 nm. It has been observed that the maximum absorption peak shifts towards the lower wavelength with increasing film thickness. This suggests the increase in the band-gap with the increasing thickness. The overall absorbance has been increased with the film thickness. This is because of the reason that in case of thicker films more atoms are present in the film so more states will be available for the photons to be absorbed. Fig 7. shows the optical reflectance spectra for ZnS thin flms. The reflectance has been found by using the relationship:

$$R + T + A = 1 \quad (5)$$

The reflectance of ZnS thin films is small in the near infrared and visible region. The over all reflectance of the film increases with the film thickness.

For normal reflectance [11], we have,

$$R = (n-1)^2 / (n+1)^2 \quad (6)$$

where R is the normal reflectance; using the above relation the refractive index, n was determined.

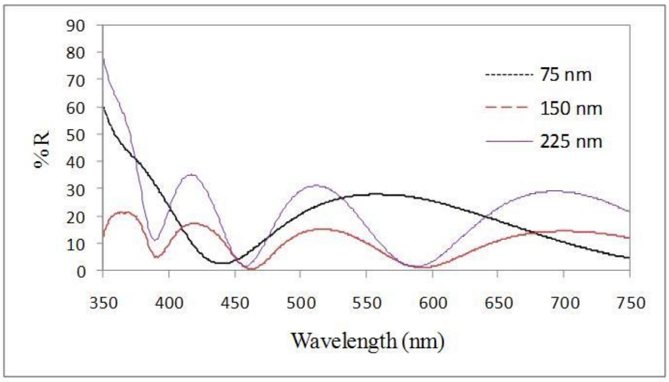

Figure 7 Reflectance versus wavelength of incident radiation.

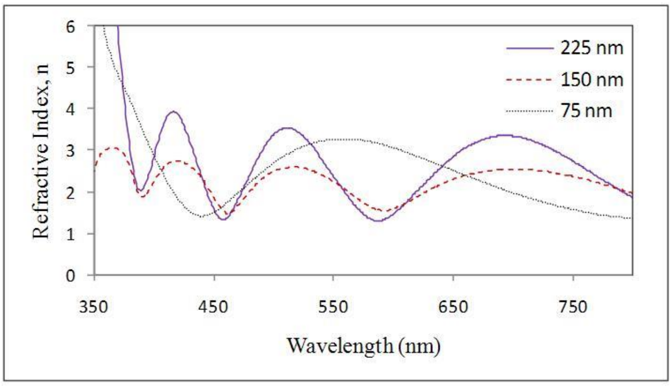

Figure 8 Refractive index versus incident photon energy.

Fig 8. shows the variations in the refractive index with the incident photon wavelength. The increase in the film thickness results in the overall increase in the refractive index. This increase is due to the overall increase in the reflectance with the film thickness which is consistent with the well-established result that the crystallinity of the polycrystalline films improves on increasing thickness. Better crystallinity of the films i.e. larger grain size leads to the higher value of n [12], which in turn increases the optical reflectance. Thus, on increasing of thickness, decrease in the optical transmittance may be attributed to the larger grain size of the films.

The peak value of the refractive index for the ZnS thin films of various thickness vary in the range of 1.52 to 3.84, which is in good agreement with the value 2.62 reported by I. C. Ndukwe [13].

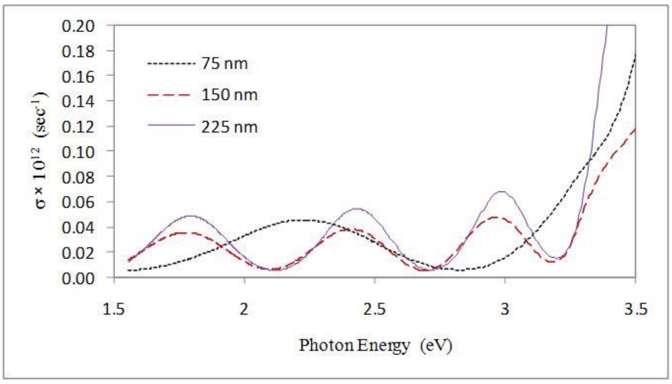

Figure 9 Optical Conductivity versus incident photon energy.

Fig 9. shows the variation of optical conductivity with the incident photon energy. The optical conductivity was determined using the relation [13]

$$\sigma = \alpha n c / 4\pi \quad (7)$$

where c is the velocity of light.

The enhanced optical conductivity at the lower wavelengths is due to the high absorbance of the films in that region.

3. CONCLUSIONS

Zinc sulfide (ZnS) thin films of different thickness were deposited on glass substrate at 50 °C temperature and high vacuum using resistive heating technique. The structural and optical characterization of film investigated include their X-ray Diffraction, absorbance / transmittance / reflectance spectra, band gap, refractive index and optical conductivity. The films were found to exhibit high transmittance (60-95%), low absorbance and low reflectance in the visible region up to 750 nm. However, the absorbance of the films was found to be high in the ultra violet region with peak around 360 nm. The thickness (Using quartz crystal) of various films ranges from 75 nm to 225 nm. The band gap measured was found to be in the range 3.25 eV to 3.48 eV. ZnS films at various annealing temperatures have a hexagonal structure with a preferred orientation of (111). The value of optical conductivity is in the range of $(0.02 - 0.2)\times10^{12}$ sec^{-1} at room temperature.

References

[1] P. Y. Feng, L-Q. Fa, C-G. Wang, Experimental and Theoretical NANOTECHNOLOGY 3 (2019) 169
[2] W.H. Bloss, F. Pfisterer, H.W. Schock, Avances in Solar Energy, An annual review of research and development, 4 (1988) 275
[3] Y.F. Nicolau, M. Dupuy, M. Brunel, J. Electrochem. Soc., 137 (1990) 2915
[4] E. Marquerdt, B. Optiz, M. Scholl, M. Henker, J. Appl. Phys. 75 (1994) 8022
[5] M.A.Hasse,J.Qiu,J.M.DePuydt,H.Cheng, Appl. Phys. Lett. 59 (1991) 1272
[6] K. Hirabayashi, H. Kozawaguchi, Jpn. J. Appl. Phys. 25 (1986) 711
[7] Guinier, X-Ray diffraction, Freeman,San Francisco,CA, USA (1963)
[8] J. P.Borah, J.Barman, K.C.Sarma, Chalcogenide Let. 59 (2008) 201
[9] P.K. Ghosh,M.K. Mitra, K.K. Chatttopadhyay, Nanotechnology 16 (2005) 107
[10] K. Ramamoorthy, C. Sanjeeviraja, M. Jayachandran, K. Sankaranarayanan, P. Bhattacharya, L. M. Kukreja, J. Cryst. Growth, (2001) 226

[11] J. I. Gittleman, E.K. Sichel, Y. Arie, Sol. Energy Mater. 1 (1979) 93
[12] K. Senthil, D. Mangalaraj, Sa. K. Narayandass, and Sadao Adachi, Mat. Sci. Eng. B 53 (2000) 78
[13] I. C. Ndukwe, Solar energy Materials and Solar Cells 40 (1996) 123